Conductance of molecular wires: Analytical modeling of connection to leads

Alexander Onipko
Department of Physics, IFM, Linköping University, S-581 83 Linköping, Sweden

Yuri Klymenko
Space Research Institute, Kiev 252022, Ukraine

Lyuba Malysheva
Bogolyubov Institute for Theoretical Physics, Kiev 252143, Ukraine
(Received 1 June 1999; revised manuscript received 24 November 1999)

The on-top and on-hollow connections of a molecule to leads are studied in the context of the single-molecule conductance measured by STM-related techniques. In the framework of the Landauer-Büttiker approach, the lead effects on the electrical properties of metal-molecular heterojunctions are expressed in terms of the spectral density (SD). The exact analytical expression of this quantity is obtained for n-dimensional ($n=1$, 2, 3) semi-infinite tight-binding leads. It has been used to examine the SD energy dependence in three and one dimensions. In most realistic cases, SD is shown to be an asymmetric (with respect to the Fermi level) function of energy which is pronouncedly distinctive from the related local density of states (LDOS) on the metal surface. For different models of molecule-to-metal connection, the LDOS on an adsorbed atom, as well as the parent LDOS on a molecular tip-facing atom and respective transmission spectrum (TS) are discussed in detail. The LDOS and TS are exemplified by the π system of 4-aminothiophenol. The approach developed is applicable straightforwardly to a fully analytical description of electrical current through conjugated oligomers with arbitrary length and chemical structure of monomers.

I. INTRODUCTION

Recent development of new techniques for fabricating and evaluating atomic and molecular scale devices has made it possible to measure and control the conductance of single molecules.[1] The strong experimental interest in the emerging field of molecular electronics is accompanied by an increasing theoretical effort aimed at understanding of the relationship between the electronic structure of molecules used to close an electric circuit, the nature of the molecule-to-metal electronic coupling and the observed current-voltage (I-V) characteristics. To describe the atomic/molecular conductance in a typical scanning tunneling microscope (STM) and quantum point contact arrangements, a variety of approaches based on analytical modeling,[2–6] semiempirical[7–9] and more elaborate *ab initio* and density functional calculations[10–12] (see also references therein) has been invented.

Mujica *et al.*[2] proposed an experimentally sound analytical theory of molecular conductance. They showed that the zero-temperature zero-bias ballistic conductance, that is just $2e^2/h$ times the transmission coefficient $T(E)$ (taken at the Fermi energy $E=E_F$) (Refs. 13–15) can be put in a convenient factorized form

$$T(E)=4\Delta_1(E)\Delta_N(E)|G_{1,N}(E)|^2 \qquad (1)$$

expressing the linear response of the junction to the applied voltage in terms of the lead spectral density $\Delta_{1(N)}(E)$ and the Green function matrix element $G_{1,N}(E)$ referred to the molecule binding sites 1 and N. In the latter quantity the molecule-metal interaction is included exactly making it dependent on $\Delta_{1(N)}(E)$ which is determined by a combination of the (semi-infinite lead) Green function matrix elements associated with the metal surface atoms connected to the molecule.

The approach which has led to Eq. (1) is, in essence, a variation on that described by Caroli *et al.*[16] Similar equations have been obtained afterwards by several authors in the framework of different techniques and in different contexts including the cases of multichannel transmission and interacting electrons. The relevant literature is too large to be reviewed here. Some basic concepts associated with Eq. (1) are discussed for example, in Ref. 17 where an extended citation is given.

Equivalents of Eq. (1) have been extensively used as a tool for studying the molecular conductance.[2–9] Nevertheless a variety of scanning tunneling spectroscopy (STS) data on substrates coated by self-assembled molecular monolayers has not yet received an adequate explanation. In particular the role of metal-molecule interfaces in forming the current across molecular monolayers is far from well understood. In terms of Eq. (1) this problem concerns the spectral density which determines the perturbation of the molecular spectrum by the interaction with the leads.

The main contributions of this paper are as follows. (i) The exact analytical expression of the spectral density for a three-dimensional (3D) lead modeled by a cubic semi-infinite lattice with an arbitrary number of atoms in the surface and subsurface layers interacting with the molecule. (ii) An analysis of the real and imaginary parts of the effective molecule-to-metal coupling as functions of energy for the on-top and on-hollow placements of the molecule end atom on the contacting surface. (iii) The use of the on-top and on-hollow models of the molecule-to-metal connection

(chemisorption) to examine the adsorbed atom and protrusion effect on the local density of states of the ideal surface. In a way the work contributes to the chemisorption theory where the analytical results have mostly been restricted to one-dimensional (1D) models.[18,19]

Since the origin of Eq. (1) is important for the understanding of the results of this work, a very compact and rigorous derivation of the transmission coefficient is first given in Sec. II. Section III proceeds with a brief discussion of STM-oriented approximations of the exact formula for the transmission coefficient. It introduces the local density of states on the outermost atom of a chemisorbed molecule, a chainlike surface protrusion, and an adsorbed atom. Section IV is central in this presentation. It specifies the on-top and on-hollow connections of a molecule (protrusion or adsorbed atom) to one- two-, and three-dimensional leads. The energy dependence of effective molecule-to-metal coupling is examined in 3D and 1D cases. For the latter, the exact analytical expression of the Newns chemisorption function[19,20] is generalized to include a subsurface atom. The asymmetry of the energy dependence of effective coupling with respect to the Fermi level in the tight-binding band is shown to be a common property. The physics of the asymmetry is explained in terms of Feynman pathways in electron-transmission events. Section V exemplifies the tip and substrate local densities of states, and the transmission spectrum. Methodologically it presents a self-contained scheme for calculating I-V characteristics on the basis of a fully analytical description which recently has been used for the interpretation of real experiments.[21] The discussion is concluded with Sec. VI while the mathematical details of the basic equations are arranged in three appendixes.

II. TRANSMISSION COEFFICIENT

The Landauer-Büttiker theory[13–15] relates the elastic conductance of a junction to the probability that an electron with the energy E injected in one ideal lead [here the substrate (s) or tip (t)] will be transmitted to another lead through a scattering region [here a molecule (m) and its contacts with the leads]. The transmission probability (or coefficient) is thus the principal quantity to be found. This task always requires some assumptions. In our model of metal-molecular heterojunctions, these are as follows.

Firstly, we assume that in the absence of the interaction between the substrate/tip and molecule the eigenstates Ψ^a of the Hamiltonian operator $\hat{H}^a$ of the substrate, tip, and molecule ($a=s$, t, and m, respectively) can be expanded in a series of the respective basis set of atomic orbitals $|\mathbf{r}\rangle$

$$\Psi^a = \sum_{\mathbf{r}\in\{\mathbf{r}\}_a} \psi^a_{\mathbf{r}} |\mathbf{r}\rangle, \tag{2}$$

where $\mathbf{r}$ denotes discrete coordinates of the $\mathbf{r}$th atom in either of the subsystems.

Secondly, $\hat{H}^s$ and $\hat{H}^t$, which describe the regions s and t, are treated as free electron Hamiltonians of semi-infinite cubic lattices with the electron on-site energy ε_a and nearest-neighbor electron-transfer interaction L_a, $a=s$, t. The tip-to-substrate drop of the applied potential U is taken into account as a uniform shift of the site energies by value of $eU_{s(t)}$ so that $U_t - U_s = U$. The operator $\hat{H}^m$ needs to be specified only at the stage of conductance analysis for a concrete molecule.

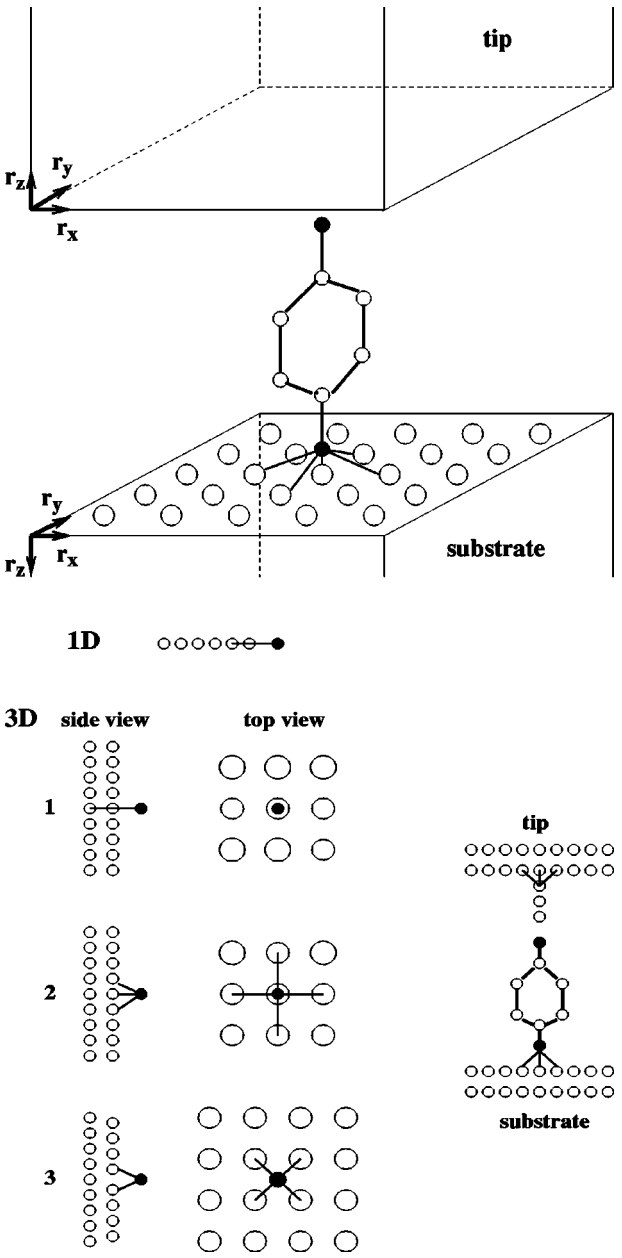

FIG. 1. A schematic representation of substrate-(chemisorbed molecule)-tip structure (up) and possible connections of the molecule end-atom (or chainlike protrusion) to the substrate or tip. Both substrate and tip are semi-infinite (in r_z direction) cubic lattices with (001) surface planes of $\mathcal{N}\times\mathcal{N}$ atoms facing each other; separate coordinate systems used for the subsystems are shown by the axis unit vectors; for the substrate and tip $r_{x(y)}=1,2,\ldots\mathcal{N}$, $r_z=1,2,\ldots\infty$. In the lower-right-hand-side corner: a side view of protrusion (molecule) connection with tip (substrate), as is prescribed by model **2**.

And finally we consider a simplified model of metal-molecular interaction which involves only two of all molecule atoms. For the convenience of further use, the coordinates of these ''binding'' atoms are denoted as 1_X and N_Y. The interaction operator is then given by

$$\hat{V}=\sum_{\mathbf{r}\in\{\mathbf{r}\}_s} V^s_{1_X,\mathbf{r}}|1_X\rangle\langle\mathbf{r}|+\sum_{\mathbf{r}\in\{\mathbf{r}\}_t} V^t_{N_Y,\mathbf{r}}|N_Y\rangle\langle\mathbf{r}|+\text{H.c.}, \quad (3)$$

with $V^s_{1_X,\mathbf{r}}$ ($V^t_{N_Y,\mathbf{r}}$) denoting the substrate-molecule (tip-molecule) coupling constants. Without any loss of generality these constants are supposed to be real and to have nonzero values for atoms lying at the substrate and tip x,y surface or subsurface monatomic layers; $\mathbf{r}=(r_\perp,r_z)$, $r_\perp=(r_x,r_y)$, see Fig. 1, and r_z runs over an arbitrary but bounded number of monolayers.

As mentioned in the introduction, the derivation of the transmission coefficient is well known. Due to simplifying model assumptions, this principal quantity is obtained here in a fully analytical form via solving the Lippman-Schwinger equation with the Hamiltonian $\hat{H}^s+\hat{H}^t+\hat{H}^m+\hat{V}$ that yields (see Appendix A)

$$T(E_F)=4A^{\mathcal{I}}_s(E_F)A^{\mathcal{I}}_t(E_F)|G_{1_X,N_Y}(E_F)|^2, \quad (4)$$

which is nothing else but Eq. (1) in the present notations.

In Eq. (4), the matrix element of the system Green function $G_{1_X,N_Y}(E_F)$ refers to the 1_Xth and N_Yth molecular atoms whose on-site energies are perturbed by the interaction with the substrate and tip. Its explicit expression in terms of the substrate and tip spectral densities and the molecular Green function is given in Eq. (A6) and exemplified by model calculations in Sec. V. The effective coupling between the molecule and substrate (tip) is represented as a simple sum of known functions

$$A^{\mathcal{I}}_{s(t)}(E_F)=\frac{1}{|L_{s(t)}|}\sum_{j_\perp}{}' \sin k_{j_\perp} \times\left(\sum_{\mathbf{r}\in\{\mathbf{r}\}_{s(t)}}\frac{\sin k_{j_\perp}r_z}{\sin k_{j_\perp}}\chi_{j_\perp}(r_\perp)V^{s(t)}_{\mathbf{r},1_X(N_Y)}\right)^2, \quad (5)$$

where the prime indicates that summation is performed only over the propagating modes of transverse electron motion in a semi-infinite cubic lattice with the $\mathcal{N}\times\mathcal{N}$ cross-section coinciding with (001) plane of the metal-molecule interfaces. The latter is described by $\chi_{j_\perp}(r_\perp)=[2/(\mathcal{N}+1)]\sin[\pi j_1 r_x/(\mathcal{N}+1)]\sin[\pi j_2 r_y/(\mathcal{N}+1)]$, j_1, $j_2=1,2,\ldots,\mathcal{N}$. In Eq. (5) $k_{j_\perp}$ stands for the electron wave vector of the transmitted mode $j_\perp=(j_1,j_2)$; these three quantum numbers are related by the energy conservation law (A10).

For the models of molecule-to-metal connections involving few metal atoms, the convergence of the sum with the increase of $\mathcal{N}$ is very quick. Except probably some energy values, to obtain $\mathcal{N}$-independent results, one can safely use a 50×50 atoms plane. In the case of very sharp dependence $A^{\mathcal{I}}_{s(t)}(E)$ on E, the use of a somewhat larger $\mathcal{N}$ may be necessary in a small energy interval. Hence from the computational point of view, the influence of various factors which play a role can be examined very easily. In particular, the difference between one-, two-, and three-dimensional models of a lead can be conveniently compared. This is to be discussed in Sec. IV.

III. STM-RELATED APPROXIMATIONS

The above consideration is free of any restrictions with regard to the values of coupling constants. To make clear references to the STM theory, we briefly discuss the particular case of one strong (with the substrate) and one weak (with the tip) molecule-metal interaction which is equivalent to the Bardeen approximation.[22] Particular attention will be paid to the conditions under which the transmission coefficient is expressed in terms of the local density of states (LDOS) on the tip-facing molecular atom (i.e., the substrate LDOS) and the tip LDOS.

A. Substrate local density of states

The conductance exhibited by conjugated molecules in STM experiments is, as a rule, by orders of magnitude smaller than that associated with a single spin degenerated level, i.e., $2e^2/h$ that corresponds to the unit transmission. The analysis of Eq. (4) shows that the unit transmission is only attainable in completely symmetric systems.[6] This is unlikely to be the case in the above mentioned experiments, since by its one end-atom the molecule is usually chemisorbed on a substrate, while the opposite end of the molecule faces an STM tip. An explanation of the low conductance can therefore be seen, in the weakness of the tip-molecule coupling controlled by the through-air tunneling in comparison with the substrate-molecule interaction that results in the creation of a chemical bond.[23]

If $|A_t|\ll|A_s|$, the exact expression (4) with $G_{1_X,N_Y}(E_F)$ defined in Eq. (A6) transforms into

$$T(E_F)=4\pi A^{\mathcal{I}}_t(E_F)\rho_s(E_F), \quad (6)$$

where the quantity

$$\rho_s(E_F)=\frac{1}{\pi}\frac{A^{\mathcal{I}}_s(E_F)[G^m_{1_X,N_Y}(E_F)]^2}{[1-A^{\mathcal{R}}_s(E_F)G^m_{1_X,1_X}(E_F)]^2+[A^{\mathcal{I}}_s(E_F)G^m_{1_X,1_X}(E_F)]^2}=-\frac{1}{\pi}\text{Im}\,G_{N_Y,N_Y}(E_F), \quad (7)$$

with $A_s^{\mathcal{R}}(E)=\pi^{-1}P\int_{-\infty}^{+\infty}A_s^{\mathcal{I}}(E')/(E-E')dE'$, has the meaning of the LDOS on atom N_Y of the molecule which is chemisorbed on the substrate surface in the absence of the tip; the notation $G^m_{n,n'}(E_F)=\langle n|(E_F-\hat{H}^m)^{-1}|n'\rangle$ is used for the molecular Green function matrix elements. The second equality in Eq. (7) can be proved by using the relations between the Green functions of the substrate and molecule and that related to the composed system: substrate plus molecule.[24]

The proportionality of transmission coefficient (i.e., Ohmic current) to the LDOS of probed sample which is stated by Eq. (7) reconfirms the corner stone of the Tersoff and Hamman STM perturbative theory.[25] However according to this equation $T(E_F)$ is not proportional to the LDOS on a tip surface atom $\rho_t(E_F)$ unless there is the only one which interacts with the molecule, i.e., $V^t_{\mathbf{r},N_Y}=\delta_{\mathbf{r},\mathbf{r}_0}V$. In such a case $A_t^{\mathcal{I}}(E_F)=\pi V^2\rho_t(E_F)$ so that

$$T(E_F)=4\pi^2V^2\rho_t(E_F)\rho_s(E_F). \tag{8}$$

We now specify the expression of the tip LDOS.

B. Tip local density of states

Literally the definition of $A^{\mathcal{I}}_{s(t)}(E_F)$ given in Eq. (5) refers to plane substrate and tip surfaces without any imperfections. The tip LDOS on the (001) surface of a semi-infinite cubic lattice can be obtained from that equation and takes the form

$$\rho_t(E_F)=\frac{4}{\pi(\mathcal{N}+1)^2|L_t|}\sum_{j_1,j_2=1}^{\mathcal{N}}{}' \sin(k_{j_1,j_2}), \tag{9}$$

where j_1 and j_2 are odd numbers only [see Appendix A and Eq. (11)].

A likely protrusion on the tip surface can be taken into account as follows. Suppose that on the otherwise ideal surface there is a single imperfection consisting of one or a few atoms in a row, as illustrated in Fig. 1. Such a structure can be considered as a ''molecule'' m' chemisorbed on the tip surface. Let also the tip-molecule interaction be dominated by only one coupling constant V that corresponds to the outmost atom of the protrusion apex. Then as can easily be shown, the expression of $\rho_t(E_F)$ in Eq. (8) is given by the expression (7) with $A_s^{\mathcal{I}}(E_F)\to A_t^{\mathcal{I}}(E_F)$ and $G^m(E_F)\to G^{m'}(E_F)$. Thereby the definition of the former quantity does not change but refers to the effective coupling between the first of the atoms lying out of the tip surface plane. Correspondingly the labeling of $G^{m'}(E_F)$ components refers to the two particular atoms in the protrusion chain, namely the closest to (the 1_Xth) and the most remote from (the N_Yth) the tip surface. Thus defined Eq. (8) describes the electron transmission between two arbitrary molecules m and m' chemisorbed on the substrate and tip surfaces and facing each other with their end atoms.

In the case of only one extra atom on the tip surface, i.e., $G^{m'}_{1_X,1_X}(E_F)=G^{m'}_{N_Y,N_Y}(E_F)=G^{m'}_{1_X,N_Y}(E_F)=(E_F-\varepsilon_t-eU_t)^{-1}$, the expression of the LDOS on the adsorbed atom is especially simple

$$\rho_t(E_F)=\frac{1}{\pi}\frac{A_t^{\mathcal{I}}(E_F)}{[E_F-\varepsilon_t-eU_t-A_t^{\mathcal{R}}(E_F)]^2+[A_t^{\mathcal{I}}(E_F)]^2} \tag{10}$$

showing a likely resonance-type character of the tip LDOS. Of course it cannot pretend to reproduce the electronic structure of real tips; the task requires a much more sophisticated modeling such as that developed for example, by Vázquez de Parga *et al.*,[26] see also references therein. However it reflects the essential factors responsible for the formation of tip LDOS resonance structure which will be discussed in Sec. V.

There are two more points to note regarding the equations represented above. Firstly, it is that electron tunneling between the tip and molecule can be included in Eq. (8) by setting $V=V_0\exp(-\hbar^{-1}\sqrt{2m^*(\Phi-E_F)}l)$, where m^* is the effective electron mass, l is the tip-molecule shortest distance, and Φ represents the work function of the tip or substrate with a proper account for the substrate-tip potential difference. The approximation of the transmission coefficient by a product of the sample and tip LDOS multiplied by the WKB exponential factor has been used in many studies. In particular Lang[27] has discussed the tunnel current between two planar metal electrodes, each having an adsorbed atom on its surface. Secondly, Eqs. (7), (8), and (10) imply that the resonance type dependence of the transmission on energy is governed by both the substrate LDOS and tip LDOS. These, as well as the energy dependence of the tip-substrate coupling via tunneling across the air gap, are important (and unavoidable) factors in STS experiments on molecular monolayers which can thus be reasonably modeled by a simple yet physically rich formula.

IV. MODELS OF THE MOLECULE-TO-METAL CONNECTION

In order to be used for practical estimates, Eq. (4), as well as its approximations (6) and (8), require specifying assumptions regarding the coupling constants. Here we discuss three particular models of the interaction between the metal atoms and end atom of the molecule (or protrusion); see Fig. 1. Two of them refer to the on-top position, i.e., the end atom is in front of metal atom (in the middle of the surface, $\mathcal{N}$ is odd). And the third is a model of on-hollow chemisorption where the molecule-terminating atom faces the center of the square between four surface atoms ($\mathcal{N}$ is even).

In this and subsequent sections, there is no need to preserve s and t labeling. By no means does this imply that the two leads must be of identical metals. Also without any change in notations, $A^{\mathcal{I}}(E)$ and $A^{\mathcal{R}}(E)$, as well as (negative) coupling constants will be expressed in units of $|L|$.

A. On-top coupling

1. Model 1

This model assumes that one surface atom and a subsurface atom next to it are involved in the metal-molecule interaction characterized by coupling constants V_1 and V_2, respectively. Then Eq. (5) may be rewritten as the following [compare with Eq. (9)]:

$$A^{\mathcal{I}}(E)=\frac{4}{(\mathcal{N}+1)^2}\sum_{j_1,j_2=1}^{\mathcal{N}}{}' \sin(k_{j_1,j_2})\sin^2\frac{\pi j_1}{2}\sin^2\frac{\pi j_2}{2} \times(V_1+2V_2\cos k_{j_1,j_2})^2. \tag{11}$$

For obvious reasons, this is the only model that admits a one-to-one comparison of the molecule-to-lead connection in one, two, and three dimension.

In the 1D case, $\mathcal{N}=1$ and $k_{j_1,j_2}\to k$. Hence there is no summation in Eq. (11). Therefore with regard to the energy dependence on the wave vector in one dimension, $E=\varepsilon-2|L|\cos k$ (the applied potential is included into the site energy) the expressions of $A^{\mathcal{I}}(E)$ and $A^{\mathcal{R}}(E)$ are accessible in an analytical form. For the former Eq. (11) gives

$$A^{\mathcal{I}}(E)=\left(V_1-V_2\frac{E-\varepsilon}{|L|}\right)^2\sqrt{1-\frac{(E-\varepsilon)^2}{4L^2}}, \tag{12}$$

if $|E-\varepsilon|\leqslant 2|L|$, and $A^{\mathcal{I}}(E)=0$ otherwise. And for the real part of effective coupling we obtain from Eq. (A12)

$$A^{\mathcal{R}}(E)=Q(E), \tag{13}$$

if $|E-\varepsilon|\leqslant 2|L|$, and

$$A^{\mathcal{R}}(E)=Q(E)-\mathrm{sgn}(E-\varepsilon)\times\left(V_1-V_2\frac{E-\varepsilon}{|L|}\right)^2\sqrt{\frac{(E-\varepsilon)^2}{4L^2}-1}, \tag{14}$$

if $|E-\varepsilon|>2|L|$, where

$$Q(E)=\frac{E-\varepsilon}{2|L|}\left(V_1-V_2\frac{E-\varepsilon}{|L|}\right)^2+2V_1V_2-V_2^2\frac{E-\varepsilon}{|L|}. \tag{15}$$

The above equations with $V_2=0$ reconfirm an old result of Newns[20] who found $A^{\mathcal{I}}(E)=V_1^2\sqrt{1-(E-\varepsilon)^2/(4L^2)}$, $A^{\mathcal{R}}(E)=[V_1^2/(2|L|)](E-\varepsilon)$, if $|E-\varepsilon|\leqslant 2|L|$, and $A^{\mathcal{I}}(E)=0$, $A^{\mathcal{R}}(E)=V_1^2[(E-\varepsilon)/(2|L|)-\mathrm{sgn}(E-\varepsilon)\times\sqrt{(E-\varepsilon)^2/(4L^2)-1}]$, otherwise. In that case $\pi^{-1}A^{\mathcal{I}}(E)=\rho(E)$ has the meaning of the LDOS on the end atom of a semi-infinite tight-binding chain. [In the chemisorption theory, $A^{\mathcal{I}}(E)$ is also called the chemisorption function.[19]] Just that expression of $A^{\mathcal{I}}(E)$ taken at $E=\varepsilon$ (i.e., $A^{\mathcal{I}}=V_1^2$ and hence, $A^{\mathcal{R}}=0$) was used in Ref. 2, to discuss the linear conductance properties on the basis of 1D model of metal-molecular junctions.

The right hand side of Eq. (12) where the molecule end atom interacts with one ($V_1\neq 0$, $V_2=0$) and two ($V_1,V_2\neq 0$) atoms of 1D lead is shown in Fig. 2. The integral spectral density increases/decreases in proportion with $V_1^2+V_2^2$

$$\frac{1}{\pi}\int_{-\infty}^{+\infty}A^{\mathcal{I}}(E')\mathrm{d}E'=V_1^2+V_2^2 \tag{16}$$

(E' is in units of $|L|$). To cancel this effect, all curves $A^{\mathcal{I}}(E)$ are multiplied by factor $(V_1^2+V_2^2)^{-1}$. For the 3D models integral (16) can also be calculated explicitly (as shown in Appendix B).

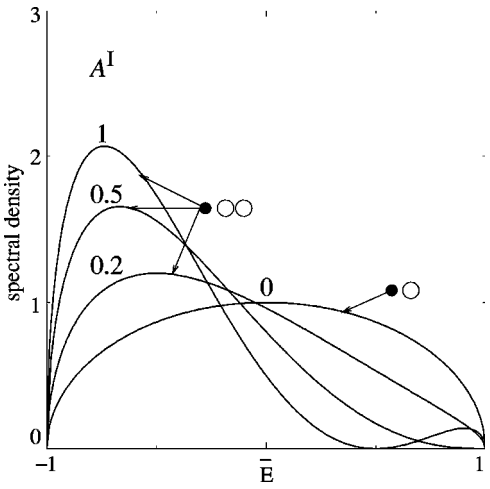

FIG. 2. Imaginary part of the effective coupling [Eq. (12)] normalized to the integral spectral density $V_1^2+V_2^2$. $\bar{E}$ denotes $(E-\varepsilon)/2|L|$; $V_2/V_1=0$, 0.2, 0.5, and 1; V_1 and V_2 are dimensionless (in units $|L|$) parameters of the interaction between the molecule binding atom (filled circle) and, respectively, ''surface'' and next to it atoms (unfilled circles) of 1D semi-infinite lead. If $0<V_2/V_1<0.5$, $A^{\mathcal{I}}(\bar{E})$ has one maximum at $\bar{E}_+$, and if $V_2/V_1>0.5$, there are two maxima at $\bar{E}_+$ and $\bar{E}_-$; $\bar{E}_\pm=(-1\pm\sqrt{1+96V_2^2/V_1^2})/(12|V_2/V_1|)$, $0\leqslant\bar{E}_+<\sqrt{2/3}$, and $-1\leqslant\bar{E}_-<-\sqrt{2/3}$. Interaction V_2 breaks the symmetry of $A^{\mathcal{I}}(\bar{E})$. The symmetric curve ($V_2=0$) is just π times LDOS on the end atom of a semi-infinite chain.

A basic distinction between the Newns chemisorption function and its more general definition given in Eq. (12) [see also Eq. (A.7)] is that the latter includes a nondiagonal component of the Green function and thus, $A^{\mathcal{I}}(E)$ cannot be interpreted in terms of the LDOS if $V_2\neq 0$. The asymmetry of the spectral density as a function of energy is entirely due to the nondiagonal matrix element of the Green function that implies the interference origin of the effect. The difference between the spectral density and LDOS becomes strongly pronounced even for small ratios (V_2/V_1); see Fig. 2. As it follows from Eq. (12), for $V_1\neq 0$ function $A^{\mathcal{I}}(E)$ is symmetric with respect to $\varepsilon(=E_F)$ only if $V_2=0$. It is not symmetric otherwise. The spectral density is larger for energies lying below the Fermi energy in a half-filled band.

2. Model 2

In this model, the coupling constant V_2 describes the interaction of the binding/adsorbed atom with the atoms next to the opposite one on the surface while constant V_1 has the same meaning as in model **1**. Hence in all, there are five surface atoms involved in the interaction with the chemisorbed molecule or adsorbed atom/protrusion, see Fig. 1. For such an (on-top) model Eq. (5) transforms into

$$A^{\mathcal{I}}(E)=\frac{4}{(\mathcal{N}+1)^2}\sum_{j_1,j_2=1}^{\mathcal{N}}{}' \sin(k_{j_1,j_2})\sin^2\frac{\pi j_1}{2}\sin^2\frac{\pi j_2}{2} \times\left[V_1+2V_2\left(\cos\frac{\pi j_1}{\mathcal{N}+1}+\cos\frac{\pi j_2}{\mathcal{N}+1}\right)\right]^2. \tag{17}$$

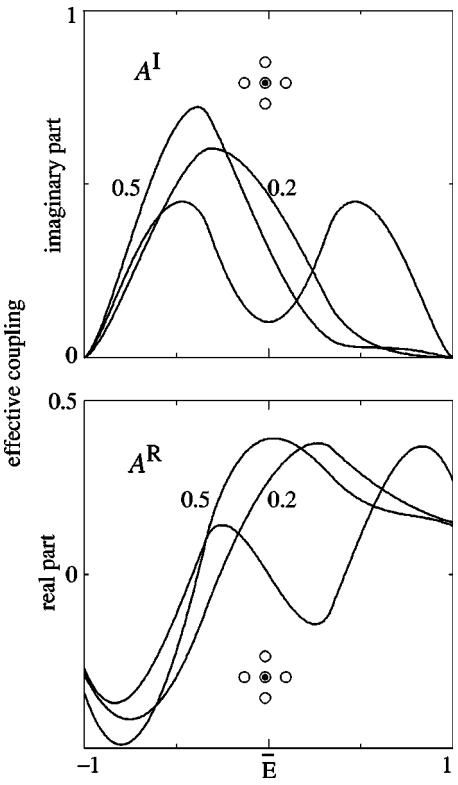

FIG. 3. Imaginary and real parts of the normalized effective coupling calculated for the 3D model **2** of on-top connection (see Fig. 1) with $V_2/V_1=0.2$ and 0.5 (labeled curves), and $V_1=0$ (unlabeled curves). Only in the special case $V_1=0$, is the imaginary (real) part of effective coupling a symmetric (antisymmetric) function of $\bar{E}=(E-\varepsilon)/(6|L|)$.

Unlike the 1D case, for 3D leads, in order to obtain an explicit expression of the dependence of effective coupling on energy, it is necessary to perform the summation analytically. This seems not to be possible. However for the given model it can be strictly proved that $(V_1\neq 0)$

$$A^{\mathcal{I}}(E-\varepsilon,V_2/V_1)=A^{\mathcal{I}}(-E+\varepsilon,-V_2/V_1), \qquad (18)$$

which implies that for arbitrary but finite values of V_2, the spectral density is a symmetric function of $E-\varepsilon$ only if $V_2=0$.

In Fig. 3, the real and imaginary parts of effective coupling are calculated for different values of V_2/V_1. As in the 1D case, to exclude the effect of the proportional increase/decrease of the integral spectral density, the dependencies $A^{\mathcal{I}}(E)$ and $A^{\mathcal{R}}(E)$ are multiplied by factor $(V_1^2+4V_2^2)^{-1}$. Basically the same effect as was just discussed in the 1D case is easily recognizable. If more than one surface atom interacts with the molecule, the nondiagonal matrix elements of the metal lead Green function come into play producing noticeable if not dramatic changes in the energy dependence of the effective coupling.

Qualitatively the role of the nondiagonal Green function components in determining the energy dependence of effective coupling is similar for the one- and three-dimensional models of molecule-to-metal connection. However, their divergence in many important details as to the shape of $A^{\mathcal{I}}(E)$ and $A^{\mathcal{R}}(E)$ curves is obvious. Therefore the predictions obtained within the 1D and 3D models regarding the electrical properties of metal-molecular heterojunctions can even be controversial. It is needless to say that the 1D model also fails to reproduce a variety of possible connections between the molecule and a real metal surface.

B. On-hollow coupling

Under the assumption that the binding/adsorbed atom is equally coupled only with four nearest-neighbor atoms on a (001) surface modeled by a square lattice, Eq. (5) takes the form

$$A^{\mathcal{I}}(E)=\frac{64V_3^2}{(\mathcal{N}+1)^2}\sum_{j_1,j_2=1}^{\mathcal{N}}{}' \sin(k_{j_1,j_2})\sin^2\frac{\pi j_1}{2} \times\sin^2\frac{\pi j_2}{2}\cos^2\frac{\pi j_1}{2(\mathcal{N}+1)}\cos^2\frac{\pi j_2}{2(\mathcal{N}+1)}. \qquad (19)$$

Changing the sign of $E-\varepsilon$ is equivalent to the following replacements in Eq. (19): $\cos^2[\pi j_1/2(\mathcal{N}+1)]\rightarrow\sin^2[\pi j_1/2(\mathcal{N}+1)]$ and $\cos^2[\pi j_2/2(\mathcal{N}+1)]\rightarrow\sin^2[\pi j_2/2(\mathcal{N}+1)]$ showing that the spectral density is an asymmetric function of $E-\varepsilon$.

It thus seems that except in some very special cases (see Fig. 3) the asymmetry of the effective coupling is its inherent property whenever more than just one surface atom is involved in the metal-molecule interaction. As an illustration, in Fig. 4 the effective coupling is calculated for on-top (models **1** and **2**) and on-hollow position. Interestingly the curves corresponding to the on-hollow connection in Fig. 4 and those that correspond to the on-top-**2** connection with $V_2/V_1=0.5$ in Fig. 3 are nearly identical. This implies that the underlying net interference effect is nearly the same.

The asymmetry of the effective coupling as a function of energy has far-going implications regarding the transmission spectrum $T(E)$ and, eventually I-V characteristics. For instance, the tip-to-substrate potential difference of the opposite signs may result in different current intensities (a diode effect). It is also noteworthy that the shape of the transmission spectrum is strongly influenced by the dependence of $A^{\mathcal{I}}$ and $A^{\mathcal{R}}$ on energy. The simple examples given above indicate that this dependence and, particularly the ratio $A^{\mathcal{I}}(E)/A^{\mathcal{R}}(E)$ may vary significantly reflecting different ways in which molecules interact with the leads to ''communicate'' with the outer world.

C. The physics of effective coupling

The asymmetric shape of $A^{\mathcal{I}}(E)$ with respect to the Fermi energy may seem to be in conflict with the symmetry of the molecule-to-metal connection models which are under discussion. A contradiction to intuitive expectations can easily be resolved by a closer look at the ''internal structure'' of effective coupling.

The binding atoms on the metal surface play the role of gate sites which let electrons in and out of the molecule in the process of transmitting electrons from one lead to another. According to Eq. (A7) the effective coupling is determined by a weighted sum of the lead Green function matrix elements which refer to the binding sites, for instance, in the case of the on-hollow

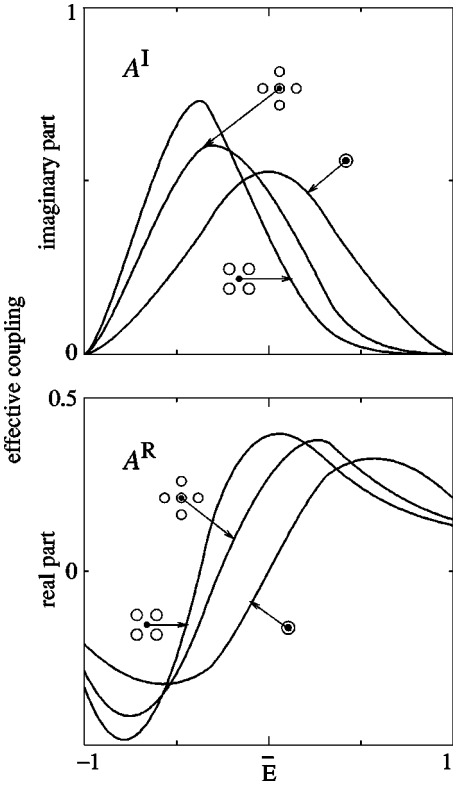

FIG. 4. The same dependencies as in Fig. 3 for 3D models of molecule-to-metal connection indicated in Fig. 1 as **1** and **2** (on-top connections with $V_2=0$ and $V_2/V_1=0.2$, respectively), and **3** (on-hollow connection); $\bar{E}=(E-\varepsilon)/(6|L|)$. As in 1D case (Fig. 2), $A^{\mathcal{I}}(\bar{E})$ is normally an asymmetric function of $\bar{E}$ whenever more than one surface atom is involved in chemisorption. Different connections of a molecule to a metal surface imply different dependencies $A^{\mathcal{I}}$ on $\bar{E}$.

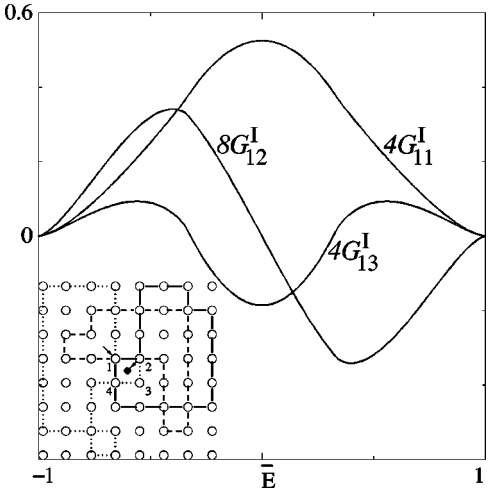

FIG. 5. The decomposition of the dimensionless spectral density into the contributions of Green function matrix elements (on-hollow connection). These contributions can be classified as ''even'' ($G^{\mathcal{I}}_{11}$, $G^{\mathcal{I}}_{13}$) and ''odd'' ($G^{\mathcal{I}}_{12}$) according to the parity of the required number of jumps in the corresponding Feynman pathways. *Inset*: top view of the contacting metal surface with four binding (gate) sites. Solid, dashed, and dotted lines show three of all the possible pathways of an electron incident from the bulk at the gate site 1 before entering the molecule through the gate site 2 (representing the contribution of $G^{\mathcal{I}}_{12}$). All such trajectories contain an odd number of elementary jumps of the electron between the nearest-neighbor atoms. $G^{\mathcal{I}}_{12}$ is therefore an odd function of $\bar{E}$.

connection, $V_3^{-2}A^{\mathcal{I}}=4G^{\mathcal{I}}_{N,N+1,1;N,N+1,1}+8G^{\mathcal{I}}_{N,N+1,1;N+1,N+1,1}+4G^{\mathcal{I}}_{N,N+1,1;N+1,N,1}$ [$G^{\mathcal{I}}_{\mathbf{r},\mathbf{r}'}\equiv-|L|\,\mathrm{Im}\,G_{\mathbf{r},\mathbf{r}'}$ defined in Eq. (A9)]. Each of these contributions to the spectral density is shown in Fig. 5 where we use simplified notations for the coordinates of the gate sites denoted as 1,2,3, and 4.

The given definition can be ''translated'' in terms of Feynman pathways as shown in the inset in Fig. 5. In such a representation, any event of the metal-molecule ''communication'' via, let us say, the binding sites 1 and 2, corresponds to all possible electron trajectories which start at site 1 and finish at 2, and *vice versa*. The contribution of all such paths into the spectral density $A^{\mathcal{I}}$ is proportional to the propagator $G^{\mathcal{I}}_{N,N+1,1;N+1,N+1,1}$. The propagators which enter the definition of the spectral density can be classified either as ''even'' or as ''odd'' according to the required number of jumps in the corresponding Feynman pathways. In the given example, the propagators $G^{\mathcal{I}}_{N,N+1,1;N,N+1,1}$, $G^{\mathcal{I}}_{N,N+1,1;N+1,N,1}$, and the like fall into the category ''even,'' whereas propagators $G^{\mathcal{I}}_{N,N+1,1;N+1,N+1,1}$ and the like are ''odd.'' An important point is that the former are even functions of $E-\varepsilon$ while the latter are odd functions of $E-\varepsilon$. Since for the majority of the molecule-to-metal connections conceived, the spectral density includes the propagators of both categories, its symmetric dependence on energy, if it occurs, should be regarded as an exotic property. For the models in focus it exists only in two special cases: $V_2=0$ and $V_1=0$ in the on-top connection models **1** and **2**, respectively.

V. ILLUSTRATIVE EXAMPLES

The aim of this section is to illustrate possible effects of the on-top and on-hollow adsorbed-atom/molecule placement on the electrode surface. From a more practical perspective this is to show how the results obtained in preceding sections can be used for modeling the STS data on electrical transport across metal-molecular junctions. At first we consider the LDOS on an adsorbed atom which may be viewed as a prototype of the tip apex atom.

A. LDOS at adatom

Energy dependencies of the adsorbed atom LDOS for the on-top (model **1** with $V_2=0$ and model **2**) and on-hollow positions are shown by solid lines in Fig. 6. These are calculated from Eq. (10). The dashed-dotted curve corresponds to Eq. (9) which gives the LDOS on the ideal (001) surface. The parameters of adsorbed atom (filled circle) are the same as for a bulk atom so that all differences in the behavior of $\rho_t(E)$ as a function of energy are connected with differences in the structure. Obviously these effects are beyond the 1D model of chemisorption since if the same atom is added to a semi-infinite chain, the latter remains unchanged.

Probably the most important message of these calculations is that in the vicinity of the Fermi energy the adsorbed atom LDOS may have a pronounced resonance-type structure which is very different from what is expected for an ideally flat Au surface.[28]

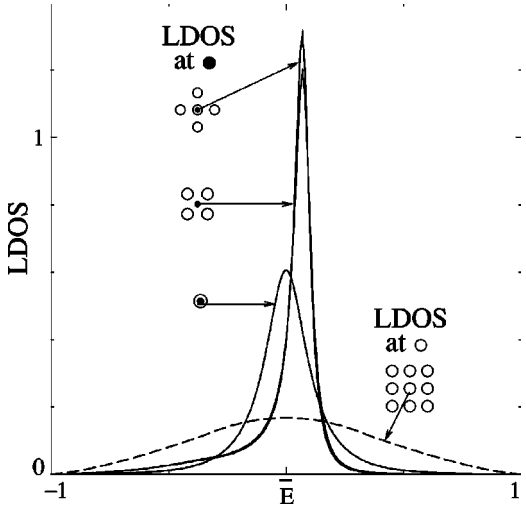

FIG. 6. LDOS on an adsorbed atom (filled circle) as described by Eq. (10) for three possible adsorbed atom-surface connections: $V_1=-1$, $V_2=0$ and $V_1=-1/\sqrt{2}$, $V_2=-1/(2\sqrt{2})$ (on-top models **1** and **2**), and $V_3=-1/2$ (on-hollow model); $\bar{E}=(E-\varepsilon)/(6|L|)$. Dashed-dotted line shows the LDOS of the ideal surface given in Eq. (9). The latter quantity is nearly constant in the vicinity of the Fermi energy ($\bar{E}=0$) while the adsorbed atom LDOS exhibits a resonance-type dependence on energy. The half-width and position of the LDOS peak are in obvious correlation with the energy dependence of effective coupling, see Fig. 4.

The narrowing of the LDOS on the adsorbed atom is, first of all, due to the change of dimensionality 3D (of the lead) to 1D (of the adsorbed atom connected to the lead). Therefore it is not surprising that the width of, e.g., model-**1** LDOS peak is roughly three times smaller than the full band width, that is in the same proportion as the ratio of the band widths in three and one dimension: $12|L|$ and $4|L|$, respectively. A similar effect is known in the electron transmission through a 1D system where the narrowing of the energy interval of the system transparency occurs. For example, in a 2D-1D-2D system with (2D-bandwidth)/(1D-bandwidth)=2, the transparency interval is two times smaller than the bandwidth of the 2D subsystem.[29]

The effect of the maximum shift and narrowing observed for the on-top-**2** and on-hollow models in Fig. 6 is in obvious correlation with the behavior of effective coupling as a function of energy. Namely for both models the LDOS redshift with respect to the Fermi energy must be nearly the same since the corresponding dependencies $A^{\mathcal{R}}(E)$ in Figs. 3 and 4 differ only slightly. Similarly higher intensity and smaller bandwidth of the on-top-**2** and on-hollow peaks is in a direct relation with a much smaller value of $A^{\mathcal{I}}(E)$ at $E\approx\varepsilon$.

Physically the red shift and sharpness of the adsorbed atom LDOS peaks in the case of on-top-**2** and on-hollow chemisorption can be understood as follows. If separated from the bulk, the adsorbed atom and surface atoms perturbed by the interaction with the former would give six and five discrete levels (i.e., δ-peaks in the LDOS) for the on-top-**2** and on-hollow models, respectively. The interaction with the bulk smears all the peaks except one of adsorbed atom which is coupled to the bulk more weakly. For the same reason it is redshifted.

Note that the interpretation given above assumes that the interaction V_2 and V_3 is comparatively weak. (In Fig. 6, the choice of these parameters is such that it maintains the same value of the integral spectral density for all three models of chemisorption.) An increase of V_2 or V_3 results in a further redshift and narrowing of the adsorbed atom resonance. In addition a new (much less intense and blueshifted) peak appears which in fact represents unresolved resonances produced by the perturbed surface atoms.

The above observations clearly indicate that the resonance structure of the adsorbed atom LDOS originates from the difference in local environment between the adsorbed and bulk atoms. For more realistic tip geometries the nature of resonances is basically the same[30] but it can be additionally influenced by the number of orbitals per atom which are forced to hybridize by a particular tip geometry,[26] and by other factors which are not taken into account in our simple models.

So the existence of tip LDOS resonances predicted at different levels of sophistication has to be considered as a likely attribute in the STS experiments. Recently it was demonstrated that I-V measurements on bare metal substrates can be dominated by the tip electronic structure with two intense peaks.[26] The resonance structure of tip LDOS is also shown to be the necessary component in order to understand a variety of STS data obtained for metal substrates coated with self-assembled molecular monolayers.[21,31]

B. LDOS at tip-facing molecular atom

An analysis of the molecular LDOS (7) requires the knowledge of the molecular Green function and thus, some specification of the molecular Hamiltonian. Of course the effects of molecule-to-metal connection on the LDOS of a particular molecule depend on details of its electronic structure. However there are many common features of how the effective coupling reveals itself in the behavior of the molecular LDOS and respective transmission spectrum (TS) as a function of energy. Here these principal conductance-related quantities are calculated for illustrative purposes using a simple model Hamiltonian of 4-aminothiophenol ($\mathrm{ATP}=\mathrm{SHC_6H_4NH_2}$). Above all, this section describes the theoretical model and calculation scheme used to model STS experiments on gold substrates covered by ATP and chemically related phenyl-based oligomer monolayers.[21]

The chemical structure of an ATP molecule is roughly sketched in Fig. 1. Such molecules can form stable self-assembled monolayers on gold[32] which have been studied by means of a STS technique.[21,33] We restrict ourselves solely to the π electron subsystem of the molecule that suggests the most efficient pathways for transmitting electrons. The π electron Hückel Hamiltonian of ATP and the molecular Green function matrix elements that one needs to calculate the transmission coefficient and/or substrate LDOS are given in Appendix C. If a sulfur-headed molecule is chemisorbed on gold, the substrate-sulfur interaction is strong but it has little effect on the rest of molecular atoms.[23,34] Therefore to choose the parameters of the model Hamiltonian, our strategy was as follows.

The π electronic structure of aniline ($=\mathrm{C_6H_5NH_2}$), which is the molecule of interest but without sulfur end

TABLE I. Molecule of aniline $C_6H_5NH_2$: energies and molecular orbital coefficients of the occupied π electron levels obtained in PM3 SCF calculations and for the Hückel model with $\alpha_C=-6.1$ eV, $\beta=-3.5$ eV, $\varepsilon_{\ddot{N}}=1$, and $\gamma_{\ddot{N}}=0.7$. The upper line of each pair of lines refers to the SCF calculations. The π electron state with zero C_1 and C_4 coefficients ($E=-9.6$ eV) is skipped.

E (eV)	C_1	C_2	C_3	C_4	C_5	C_6	N
−8.1	0.43	0.12	−0.36	−0.28	−0.36	0.12	0.66
−8.3	0.42	0.13	−0.34	−0.35	−0.34	0.13	0.66
−10.9	−0.50	−0.34	−0.01	0.38	−0.01	−0.34	0.61
−10.9	−0.48	−0.33	0.02	0.36	0.02	−0.33	0.65
−13.4	0.31	0.34	0.40	0.51	0.40	0.34	0.32
−13.4	0.33	0.35	0.40	0.48	0.40	0.35	0.31

group, has been agreed with semiempirical SCF calculations performed with the PM3 Hamiltonian (MOPAC'97 package). Table I shows a remarkably good reproducibility of the SCF results by our model Hamiltonian. With the successful set of parameters as specified in Table I, the same calculation routine has then been used to determine the sulfur parameters: the site energy 1.3β and the S-C hopping integral 0.5β, β (<0) is the C-C hopping integral within the phenyl ring. Though these parameters agree with SCF data reasonably well, they are less certain; particularly, because the effect of sulfur-substrate interaction has not been taken into account.

According to Eq. (7) the portrait of the molecular electronic structure exposed by STS of a molecular monolayer is mostly determined by two factors. These are on the one hand, the molecular characteristics and on the other hand, the energy dependence of effective coupling and the (dimensionless) coupling strength constants $\mathcal{V}_i=V_i^2|\beta|/|L|$, $i=1, 2, 3$. It is seen that any of these constants includes three independent parameters: the squared matrix element of the metal-molecule interaction divided by the characteristic scales of the metallic and molecular one-electron spectra. By using $|L|$ or $|\beta|$ as the energy unit, the number of parameters which enter the coupling strength can be reduced to the two, say, V_i in units of $|\beta|$ and the ratio $|\beta|/|L|$.

By fixing V_i and varying $|\beta|/|L|$ one can trace how the perturbation, which is identical in terms of the molecular energy scale but produced by metals with the different width of the actual free electron band, affects the display of molecular electronic structure (that is LDOS) and consequently, the transmission spectrum. To our knowledge, the LDOS and TS dependence on the parameters of molecule-to-lead connection has never been examined in such a context before, though implicitly it is present in any calculations of the conductance related properties of metal-molecular junctions.

The calculations of TS and LDOS with the use of the molecular Green function found in Appendix C have been performed for the values of coupling constants and molecular parameters indicated in figure captions. The LDOS and TS curves in Fig. 7 refer to the on-hollow position of the binding sulfur atom. The LDOS is calculated exactly (left-hand-side curves) and approximately with the use of two choices of a *constant* effective coupling $A(E)=A(\varepsilon)$. Namely, the real and imaginary parts of $A(\varepsilon)$ were prescribed to be as if they were for the on-hollow chemisorption

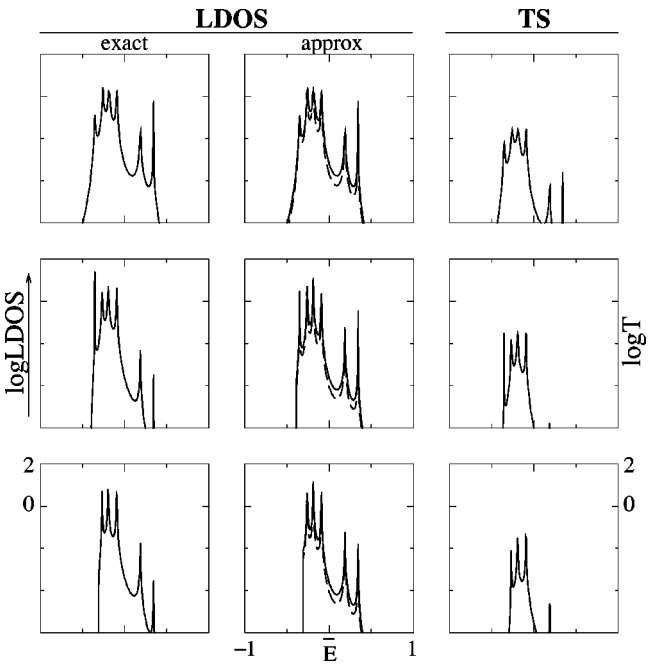

FIG. 7. The local density of states $|\beta|\rho_s(E)$ (7) and transmission coefficient for molecule $SHC_6H_4NH_2$ chemisorbed on a model substrate with sulfur atom in the on-hollow position above the (001) surface; the substrate and tip coupling constants (in units of $|\beta|$) are fixed at values $V_3=-0.25$ and -0.025, respectively. The π electronic structure parameters are $\varepsilon_S=1.3$, $\gamma_S=0.5$, and those specified in Table I. The model exact LDOS (left-hand-side column) is compared with the approximation of constant effective coupling (center column) for different values of the substrate parameters $|L|/|\beta|$ and $(\varepsilon-\alpha_C)/|\beta|$: (from top to bottom) 1 and 0; 0.4 and 0; 0.4 and 0.5; $\bar{E}=(E-\varepsilon)/(6|L|)$. The approximate curves are calculated with $A(E)=A(\bar{E}=0)$ for the on-hollow (solid line) and on-top-**1** (dashed line) models. In the latter case, $A(\bar{E}=0)=-i\pi\times\mathrm{LDOS}(E_F)$ of the surface. The LUMO (lowest unoccupied molecular orbital) and HOMO (highest occupied molecular orbital) levels correspond to the second and third peaks of LDOS (TS) from the right, respectively.

model (solid lines) and on-top-**1** model with $V_2=0$ (dashed lines). In the latter case $A^{\mathcal{R}}(\varepsilon)=0$ so that the role of other factors which influence the molecular wire performance is easier to understand. However, such an approximation appears to be only in a rough qualitative agreement with the exact results. Therefore it may be used but with a good deal of caution. In particular, it is obvious that the constant effective coupling approximation fails to reproduce the real difference between the on-top and on-hollow connections of a molecule to the substrate.

Since energetically the two models of chemisorption do not differ much,[23] both can be met in real samples. The corresponding LDOS and TS are compared in Figs. 7 and 8 which represent the on-hollow and on-top models, respectively. As one can see, distinctions between the two models are strongly pronounced even in the logarithmic scale used for drawing. In both figures, the parent LDOS on the tip-facing nitrogen atom of ATP (left-hand-side curves) can be compared with the respective TS. In the center column of Fig. 8, TS curves are calculated for the symmetric coupling (the substrate and tip coupling constants are equal, $|V_1|$

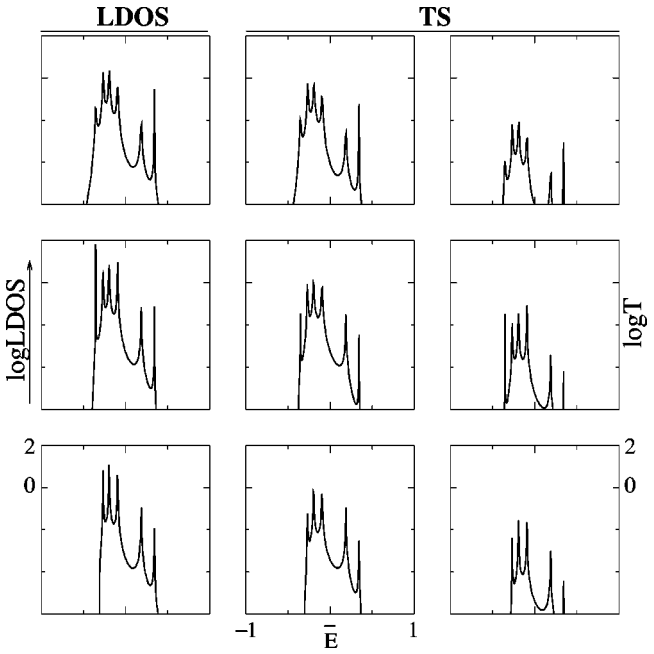

FIG. 8. In the left-hand side column, the same LDOS with the same parameters as in Fig. 7 but for the on-top placement of sulfur (model **1** with $V_1=-0.25$ and $V_2=0$). In central and right-hand side columns, TS is calculated with the same parameters as for LDOS; the tip-molecule coupling constant V_1 is equal to -0.25 (central column) and -0.025 (right-hand side column). The on-hollow and on-top chemisorption produce LDOS and TS of different shapes, in particular, differences in relative intensities of the HOMO and LUMO peaks are well distinct for the two models even in the logarithmic scale.

$=0.25$); in the right-hand-side columns $|V_3|$ (in Fig. 7) and $|V_1|$ (in Fig. 8) are set to be equal to 0.25 for the substrate, and $|V_1|=|V_3|=0.025$ for the tip.

The shape of LDOS and TS is strongly affected by the relative position of the substrate Fermi energy with respect to the molecular levels. In Figs. 7 and 8, this factor is represented by the parameter $(\varepsilon-\alpha_C)/|\beta|$. Again even in the logarithmic scale, the effect of a mismatch between E_F $(=\varepsilon)$ and α_C is well noticeable. The Fermi energies of most metals are tabulated. For Au $E_F=5.2$ eV so that with the values of α_C and β specified in Table I we have $(\varepsilon-\alpha_C)/|\beta|\approx 0.26$ which, within the present scheme, may be advised as a reasonable choice of the mismatch parameter. Unfortunately, this value as well as other model parameters cannot be unambiguously inferred from the experiment. The use of the theory is then seen in the possibility of fixing the parameters associated with the metal-molecule interaction by fitting STS data for a particular molecular monolayer and to predict changes in the current along related molecules with presumably the same characteristics of the metal-molecular interface. As demonstrated in Ref. 21, such a strategy allows us to explain in a consistent manner a variety of factors and their interplay in forming the apparent I-V relation for phenyl-based oligomers of different lengths, at different set-points of the tunnel current, and with essentially one and the same set of input parameters.

VI. CONCLUDING REMARKS

The above calculations exemplify the strongest effects of the metal-to-leads connection on the molecule ability as an electron transmitter. They also aim to illustrate the potentials of a *fully analytical modeling.* It is worthy of note that it takes seconds to obtain LDOS, TS, the respective I-V or other desired characteristics for the given π electronic structure of short molecules. Minutes are required to obtain similar data for conjugated oligomers of any reasonable length.

For this class of molecules the Green function is expressed analytically in terms of the monomer Green function.[24] Moreover for long molecular wires, the tunneling decay constant is explicitly related to the monomer electronic structure.[5,35,36] The approach is also readily applicable to the σ electron systems.[6]

A question may be raised as to the relevance of the model simplifications, in particular, the use of single particle approximation. The generalizations beyond that are likely to be possible. The simplest way is to fit the input parameters with the data of reliable semiempirical or *ab initio* calculations as it has been exemplified by calculations of the molecular subsystem.

Our model assumes only one molecular atom to be electronically coupled with each of two electrodes. And only one atomic state (atomic orbital) from the either side of the molecule is supposed to be responsible for the coupling with the source/drain electrode. Such assumptions are supported by experimental data[1,9,21] and theoretical estimates[2,4–9,11] which suggest the π electron subsystem plays the major role in maintaining the electrical current mediated by conjugated oligomers.

Further improvements are in progress. The analytical results obtained provide a helpful guide for developing more realistic models which take into account the real structure of the substrate surface (e.g., 111 surface of fcc lattice and others), which also use extended basis sets, and which go beyond the nearest-neighbor and one-particle approximations.

ACKNOWLEDGMENTS

This work was financially supported by Swedish Research Council for Engineering Sciences (TFR), and by Royal Swedish Academy of Sciences, Stockholm (KVA). The authors wish to thank Dr. L.J. Geerligs and J.J.W.M. Rosink for discussions and giving unpublished experimental data.

APPENDIX A: DERIVATION OF TRANSMISSION COEFFICIENT

For the Hamiltonian $\hat{H}^s+\hat{H}^t+\hat{H}^m+\hat{V}$ (as is defined in Sec. II) the Lippman-Schwinger equation[37] determining the scattering states outside the molecule $(\mathbf{r}\notin\{\mathbf{r}\}_m)$ takes the form

$$\psi^s_{\mathbf{r}}=\psi^{s0}_{\mathbf{r}}+\sum_{\mathbf{r}'\in\{\mathbf{r}\}_s} G^s_{\mathbf{r},\mathbf{r}'}V^s_{1_X,\mathbf{r}'}\psi^m_{1_X}, \tag{A1}$$

$$\psi^t_{\mathbf{r}}=\sum_{\mathbf{r}'\in\{\mathbf{r}\}_t} G^t_{\mathbf{r},\mathbf{r}'}V^t_{N_Y,\mathbf{r}'}\psi^m_{N_Y}, \tag{A2}$$

where

$$\psi^m_{1_X}=\sum_{\mathbf{r}\in\{\mathbf{r}\}_s} G^m_{1_X,1_X}V^s_{1_X,\mathbf{r}}\psi^s_{\mathbf{r}}+\sum_{\mathbf{r}\in\{\mathbf{r}\}_t} G^m_{1_X,N_Y}V^t_{N_Y,\mathbf{r}}\psi^t_{\mathbf{r}}, \tag{A3}$$

$$\psi^m_{N_Y}=\sum_{\mathbf{r}\in\{\mathbf{r}\}_s} G^m_{N_Y,1_X}V^s_{1_X,\mathbf{r}}\psi^s_{\mathbf{r}}+\sum_{\mathbf{r}\in\{\mathbf{r}\}_t} G^m_{N_Y,N_Y}V^t_{N_Y,\mathbf{r}}\psi^t_{\mathbf{r}}, \tag{A4}$$

$G^a_{\mathbf{r},\mathbf{r}'}=\langle\mathbf{r}|(E-\hat{H}^a)^{-1}|\mathbf{r}'\rangle$, and $\psi^{s0}_{\mathbf{r}}$ is an eigenstate of $\hat{H}^s$ describing incident and reflected electron waves in the bare substrate. To simplify notations, the indication of an explicit dependence of $\psi^{s0}_{\mathbf{r}}$, $\psi^a_{\mathbf{r}}$, and $G^a_{\mathbf{r},\mathbf{r}'}$ on the incident electron energy E and applied voltage U is omitted.

For $a=m$ the Green function matrix elements are real but for $a=s$, t, they are complex functions. However as is seen there is no infinitesimal imaginary part of energy in the substrate/tip Green function definition. Instead we use the solution of the Green function problem with the Hamiltonian of a semi-infinite lead that behaves as outgoing waves at the infinity.

By definition the transmission coefficient is determined by the amplitudes of the transmitted waves. This means that we have to find the function $\psi^t_{\mathbf{r}}$ which satisfies the above set of equations. It is easy to see that the solution to the set of Eqs. (A1) and (A2) is given by

$$\psi^t_{\mathbf{r}}=G_{1_X,N_Y}\sum_{\mathbf{r}'\in\{\mathbf{r}\}_s} V^s_{1_X,\mathbf{r}'}\psi^{s0}_{\mathbf{r}'}\sum_{\mathbf{r}'\in\{\mathbf{r}\}_t} G^t_{\mathbf{r},\mathbf{r}'}V^t_{\mathbf{r}',N_Y}, \tag{A5}$$

where

$$G_{1_X,N_Y}=\frac{G^m_{1_X,N_Y}}{(1-A_sG^m_{1_X,1_X})(1-A_tG^m_{N_Y,N_Y})-A_sA_t(G^m_{1_X,N_Y})^2} \tag{A6}$$

having the meaning of the molecular Green function matrix element referring to the 1_Xth and N_Yth atoms whose on-site energies are perturbed due to the interaction with the substrate and tip by complex energy-dependent values of

$$A_s=\sum_{\mathbf{r},\mathbf{r}'\in\{\mathbf{r}\}_s} V^s_{1_X,\mathbf{r}}G^s_{\mathbf{r},\mathbf{r}'}V^s_{\mathbf{r}',1_X},$$

$$A_t=\sum_{\mathbf{r},\mathbf{r}'\in\{\mathbf{r}\}_t} V^t_{N_Y,\mathbf{r}}G^t_{\mathbf{r},\mathbf{r}'}V^t_{\mathbf{r}',N_Y}, \tag{A7}$$

respectively. These quantities play the role of the self energy which determines the shift and broadening of molecular levels.[2,7,17]

The solution (A5) is valid for any shape and electronic structure of the substrate, tip, and molecule. To obtain its explicit form, we make further use of the model assumptions. Let the contact surfaces be $\mathcal{N}\times\mathcal{N}$ square lattices coinciding with (001) planes of s and t cubic lattices. Then,

$$\psi^{s0}_{r_\perp,r_z}=2i\sin(k'_{j'_\perp}r_z)\chi_{j'_\perp}(r_\perp) \tag{A8}$$

and

$$G^a_{r_\perp,r_z;r'_\perp,r'_z}=\frac{1}{L_a}\sum_{j_\perp} e^{ik_{j_\perp}r_z}\frac{\sin k_{j_\perp}r'_z}{\sin k_{j_\perp}}\chi_{j_\perp}(r_\perp)\chi_{j_\perp}(r'_\perp), \tag{A9}$$

if $r_z\geqslant r'_z$; for $r_z<r'_z$ in the right-hand side of Eq. (A9), the replacement $r_z\leftrightarrow r'_z$ has to be made.

In Eqs. (A8) and (A9), $a=s$, t; $k'_{j'_\perp}$ is the incident electron wave vector, $j'_\perp=(j'_1,j'_2)$ is the quantum number of the transverse electron motion described by $\chi_{j'_\perp}(r_\perp)=[2/(\mathcal{N}+1)]\sin[\pi j'_1r_x/(\mathcal{N}+1)]\sin[\pi j'_2r_y/(\mathcal{N}+1)]$; $k_{j_\perp}$ and $j_\perp$ have similar meanings for the transmitted (or reflected) electron waves.

At the given energy E, the values of $k'_{j'_\perp}$ and $j'_\perp$, as well as $k_{j_\perp}$ and $j_\perp$ are not independent since they have to satisfy the energy conservation law $E^s_{k'_{j'_\perp},j'_\perp}+eU_s=E^t_{k_{j_\perp},j_\perp}+eU_t=E$. For the leads modeled by nearest-neighbor tight-binding semi-infinite lattice the allowed values of wave vectors can be found from

$$E-eU_a=\varepsilon_a-2|L_a|\left(\cos k_{j_1,j_2}+\cos\frac{\pi j_1}{\mathcal{N}+1}+\cos\frac{\pi j_2}{\mathcal{N}+1}\right). \tag{A10}$$

The wave vector of scattered waves $k_{j_\perp}$ in Eq. (A10) takes real and imaginary ($k_{j_\perp}=\pm iq_{j_\perp}$, $k_{j_\perp}=\pi\pm iq_{j_\perp}$) values which correspond to the propagating and evanescent modes, respectively.

With regard to Eqs. (A7) and (A9), the imaginary part of the effective coupling constants $A_a=A^{\mathcal{R}}_a-iA^{\mathcal{I}}_a$ can be represented in an explicit form

$$A^{\mathcal{I}}_{s(t)}(E_F)=\frac{1}{|L_{s(t)}|}{\sum_{j_\perp}}'\sin k_{j_\perp}\times\left(\sum_{\mathbf{r}\in\{\mathbf{r}\}_{s(t)}}\frac{\sin k_{j_\perp}r_z}{\sin k_{j_\perp}}\chi_{j_\perp}(r_\perp)V^{s(t)}_{\mathbf{r},1_X(N_Y)}\right)^2, \tag{A11}$$

where the prime indicates the summation over propagating modes. Thus $A^{\mathcal{I}}_{s(t)}\neq 0$ only within the $s(t)$ electron energy band.

Note that in Eqs. (A10) and (A11), the sign of L_a (assumed to be negative) is explicitly taken into account. Hence $A^{\mathcal{I}}_a$ which is usually called the spectral density is a positively defined quantity.

The expression of $A^{\mathcal{R}}_a$ also follows from Eqs. (A7) and (A9). But actually it is not needed since as a linear combination of the retarded Green function components, the real and imaginary parts of the effective coupling must satisfy the Kramers-Kronig dispersion relation[38,39] which is discussed in many textbooks.[40,41] This means that $A^{\mathcal{R}}_a(E)$ and $A^{\mathcal{I}}_a(E)$ are related by the Hilbert transform

$$A_a^{\mathcal{R}}(E)=\frac{1}{\pi}P\int_{-\infty}^{+\infty}\frac{A_a^{\mathcal{I}}(E')}{E-E'}dE', \tag{A12}$$

where P denotes the Cauchy principal value.

Except the Green function G_{1_X,N_Y} all the quantities that determine transmitted waves are now represented in an analytical form. The substitution of expressions (A8) and (A9) in Eq. (A5) yields

$$\psi^t_{r_\perp,r_z}=\sum_{j_\perp} t_{k_{j_\perp},j_\perp;k'_{j'_\perp},j'_\perp}(r_\perp)\exp(ik_{j_\perp}r_z), \tag{A13}$$

$$t_{k_{j_\perp},j_\perp;k'_{j'_\perp},j'_\perp}(r_\perp)=\frac{2i\sin k'_{j'_\perp}}{L_t}\chi_{j_\perp}(r_\perp)\tilde{\chi}^s_{j'_\perp}\tilde{\chi}^t_{j_\perp}G_{1_X,N_Y}, \tag{A14}$$

where $\tilde{\chi}^a_{j_\perp}=\Sigma_{\mathbf{r}'\in\{\mathbf{r}\}_a}(\sin k_{j_\perp}r'_z/\sin k_{j_\perp})\chi_{j_\perp}(r'_\perp)V^a_{N_Y,r'_\perp}$. By using Eq. (A14) in the definition of the transmission coefficient

$$T=\sum_{j'_\perp}{}'\sum_{j_\perp}{}'\sum_{r_\perp}\frac{v^t_{k_{j_\perp}}}{v^s_{k'_{j'_\perp}}}|t_{k_{j_\perp},j_\perp;k'_{j'_\perp},j'_\perp}(r_\perp)|^2, \tag{A15}$$

with the group velocities ratio given by $v^s_{k'_{j'_\perp}}/v^t_{k_{j_\perp}}=|L_s|\sin k'_{j'_\perp}/(|L_t|\sin k_{j_\perp})$ one obtains Eq. (4).

Note that generalizations of Eq. (4) to the case of arbitrary number of molecular atoms interacting with the leads convert the obtained *closed* definition of the transmission coefficient into a set of equations to be solved. Equally it can be represented in the form of a product of the self-energy matrix and an *unknown* matrix of the system Green function.[17,42]

It is also noteworthy that the method of the Lippman-Schwinger equation which is used here to derive the transmission coefficient is self-contained and does not require any auxiliary quantities. The system wave function is obtained as an intermediate result. Thus the method gives the most detailed description of the system that may be difficult to attain in the framework of other approaches.

APPENDIX B: INTEGRAL SPECTRAL DENSITY

For the model **1** of on-top molecule-to-metal connection specified in Eq. (11) the integral spectral density is given by

$$\frac{1}{\pi}\int_{-\infty}^{\infty}A^{\mathcal{I}}(E)dE=\frac{4\pi^{-1}}{(\mathcal{N}+1)^2}\sum_{j_1,j_2=1}^{\mathcal{N}}\sin^2\frac{\pi j_1}{2}\times\sin^2\frac{\pi j_2}{2}\int_{|\cos(k_{j_1,j_2})|\leqslant 1}\sin(k_{j_1,j_2})\times[V_1+2V_2\cos(k_{j_1,j_2})]^2dE, \tag{B1}$$

where $\mathcal{N}$ is odd, and E (in units of $|L|$) and k_{j_1,j_2} are related by the energy conservation law (A10). Introducing a new variable of integration

$$x=\frac{\varepsilon_a+eU_a-E}{2}-\cos\left(\frac{\pi j_1}{\mathcal{N}+1}\right)-\cos\left(\frac{\pi j_2}{\mathcal{N}+1}\right),$$

we calculate

$$\int_{|\cos(k_{j_1,j_2})|\leqslant 1}\sin(k_{j_1,j_2})dE=2\int_{-1}^{1}\sqrt{1-x^2}dx=\pi, \tag{B2}$$

$$\int_{|\cos(k_{j_1,j_2})|\leqslant 1}\sin(k_{j_1,j_2})\cos(k_{j_1,j_2})dE=2\int_{-1}^{1}x\sqrt{1-x^2}dx=0, \tag{B3}$$

$$\int_{|\cos(k_{j_1,j_2})|\leqslant 1}\sin(k_{j_1,j_2})\cos^2(k_{j_1,j_2})dE=2\int_{-1}^{1}x^2\sqrt{1-x^2}dx=\frac{\pi}{4}. \tag{B4}$$

Using these results in Eq. (B1) and taking into account that $\Sigma_{j=1}^{2N+1}\sin^2(\pi j/2)=N+1$, one gets

$$\frac{1}{\pi}\int_{-\infty}^{\infty}A^{\mathcal{I}}(E)dE=\frac{4(V_1^2+V_2^2)}{(\mathcal{N}+1)^2}\sum_{j_1,j_2=1}^{\mathcal{N}}\sin^2\frac{\pi j_1}{2}\sin^2\frac{\pi j_2}{2}=V_1^2+V_2^2. \tag{B5}$$

Similarly, the calculation of the integral spectral density for the on-top-**2** model with $A^{\mathcal{I}}(E)$ given in Eq. (17) yields

$$\frac{1}{\pi}\int_{-\infty}^{\infty}A^{\mathcal{I}}(E)dE=\frac{4}{(\mathcal{N}+1)^2}\sum_{j_1,j_2=1}^{\mathcal{N}}\sin^2\frac{\pi j_1}{2}\sin^2\frac{\pi j_2}{2}\left[V_1+2V_2\left(\cos\frac{\pi j_1}{\mathcal{N}+1}+\cos\frac{\pi j_2}{\mathcal{N}+1}\right)\right]^2=V_1^2+4V_2^2, \tag{B6}$$

where the equalities $\Sigma_{j=1}^{2N+1}\cos[\pi j/(2N+2)]\sin^2(\pi j/2)=0$ and $\Sigma_{j=1}^{2N+1}\cos^2[\pi j/(2N+2)]\sin^2(\pi j/2)=(N+1)/2$ have been used.

For the on-hollow model, the integral spectral density [see Eq. (19)] is given by

$$\frac{1}{\pi}\int_{-\infty}^{\infty} A^{\mathcal{I}}(E)dE=\frac{64(V_3)^2\pi}{(\mathcal{N}+1)^2}\sum_{j_1,j_2=1}^{\mathcal{N}}\sin^2\frac{\pi j_1}{2}\sin^2\frac{\pi j_2}{2}\cos^2\frac{\pi j_1}{2(\mathcal{N}+1)}\cos^2\frac{\pi j_2}{2(\mathcal{N}+1)}$$

$$=\frac{16(V_3)^2}{(\mathcal{N}+1)^2}\sum_{j_1,j_2=1}^{\mathcal{N}}\sin^2\frac{\pi j_1}{2}\sin^2\frac{\pi j_2}{2}\left[1+\cos\frac{\pi j_1}{\mathcal{N}+1}\right]\left[1+\cos\frac{\pi j_2}{\mathcal{N}+1}\right]=4V_3^2, \tag{B7}$$

where $\Sigma_{j=1}^{2N}\sin^2(\pi j/2)=N$, $\Sigma_{j=1}^{2N}\cos[\pi j/(2N+1)]\sin^2(\pi j/2)=\frac{1}{2}$. To recall, in Eq. (B6) $\mathcal{N}$ is odd, and in Eq. (B7) $\mathcal{N}$ is even.

With the coupling constants set equal to unit the value of the integral spectral density is equal to the number of metal atoms which are in contact with the molecule.

APPENDIX C: MOLECULAR HAMILTONIAN AND GREEN FUNCTION

The π electron Hamiltonian of benzene with two hydrogens substituted by heteroatoms X and Y (in an ATP molecule these are sulfur and nitrogen) can be represented as

$$\hat{H}^m=\sum_{i=1}^{6}\left[\alpha_{\mathrm{C}}|\mathrm{C}_i\rangle\langle\mathrm{C}_i|+\beta(|\mathrm{C}_{i+1}\rangle\langle\mathrm{C}_i|+\mathrm{H.c.})\right]$$

$$+\beta\{\varepsilon_{\mathrm{X}}|1_{\mathrm{X}}\rangle\langle 1_{\mathrm{X}}|+\varepsilon_{\mathrm{Y}}|N_{\mathrm{Y}}\rangle\langle N_{\mathrm{Y}}|+[\gamma_{\mathrm{X}}|\mathrm{C}_1\rangle\langle 1_{\mathrm{X}}|+\gamma_{\mathrm{Y}}|\mathrm{C}_4\rangle\langle N_{\mathrm{Y}}|+\mathrm{H.c.}]\}, \tag{C1}$$

where $|\mathrm{C}_i\rangle$ has the meaning of the $2p_z$ atomic orbital of the ith C atom within a phenyl ring ($\mathrm{C}_7\equiv\mathrm{C}_1$), while $|1_{\mathrm{X}}\rangle$ and $|N_{\mathrm{Y}}\rangle$ refer to the heteroatom orbitals; α_{C} and $\alpha_{\mathrm{X(Y)}}$ are the Coulomb integrals (the π electron site energies) of C and X (Y) atoms, respectively; β is the resonance integral between the nearest-neighbor carbons; $\beta\varepsilon_{\mathrm{X(Y)}}=\alpha_{\mathrm{X(Y)}}-\alpha_{\mathrm{C}}$, and $\beta\gamma_{\mathrm{X(Y)}}$ is the resonance integral between C and X (Y) atoms.

For the matrix elements $G^m_{\mathbf{r},\mathbf{r}'}$ which appear in Eq. (A6), the inversion of the matrix

$$E\mathbf{I}-\beta^{-1}\mathbf{H}^m=\begin{pmatrix} E-\varepsilon_{\mathrm{X}} & \gamma_{\mathrm{X}} & 0 & 0 & 0 & 0 & 0 & 0\\ \gamma_{\mathrm{X}} & E & 1 & 0 & 0 & 0 & 1 & 0\\ 0 & 1 & E & 1 & 0 & 0 & 0 & 0\\ 0 & 0 & 1 & E & 1 & 0 & 0 & 0\\ 0 & 0 & 0 & 1 & E & 1 & 0 & 0\\ 0 & 0 & 0 & 0 & 1 & E & 1 & 0\\ 0 & 1 & 0 & 0 & 0 & 1 & E & \gamma_{\mathrm{Y}}\\ 0 & 0 & 0 & 0 & 0 & 0 & \gamma_{\mathrm{Y}} & E-\varepsilon_{\mathrm{Y}} \end{pmatrix} \tag{C2}$$

yields

$$\beta G^m_{1_{\mathrm{X}},1_{\mathrm{X}}}=[(E-\varepsilon_{\mathrm{Y}})(E^2-1)(E^2-4)-\gamma_{\mathrm{Y}}^2E(E^2-3)]\mathcal{D}^{-1}, \tag{C3}$$

$$\beta G^m_{N_{\mathrm{Y}},N_{\mathrm{Y}}}=[(E-\varepsilon_{\mathrm{X}})(E^2-1)(E^2-4)-\gamma_{\mathrm{X}}^2E(E^2-3)]\mathcal{D}^{-1}, \tag{C4}$$

$$\beta G^m_{1_{\mathrm{X}},N_{\mathrm{Y}}}=2\gamma_{\mathrm{X}}\gamma_{\mathrm{Y}}\mathcal{D}^{-1}, \tag{C5}$$

where

$$\mathcal{D}=\gamma_{\mathrm{X}}^2\gamma_{\mathrm{Y}}^2(E^2-1)-E(E^2-3)[\gamma_{\mathrm{X}}^2(E-\varepsilon_{\mathrm{Y}})+\gamma_{\mathrm{Y}}^2(E-\varepsilon_{\mathrm{X}})]+(E-\varepsilon_{\mathrm{X}})(E-\varepsilon_{\mathrm{Y}})(E^2-1)(E^2-4) \tag{C6}$$

and, to simplify the expressions of molecular Green function components, E stands for $(E-\alpha_{\mathrm{C}})/\beta$.

For ATP molecule $\varepsilon_{\mathrm{X}}\equiv\varepsilon_{\mathrm{S}}$, $\gamma_{\mathrm{X}}\equiv\gamma_{\mathrm{S}}$, $\varepsilon_{\mathrm{Y}}\equiv\varepsilon_{\ddot{\mathrm{N}}}$, and $\gamma_{\mathrm{Y}}\equiv\gamma_{\ddot{\mathrm{N}}}$ are the parameters of sulfur and nitrogen used in the main body of the paper.

[1] M. Dorogi, J. Gomez, R.G. Osifchin, R.P. Andres, and R. Reifenberger, Phys. Rev. B **52**, 9071 (1995); J.M. Tour, L. Jones II, D.L. Pearson, J.J.S. Lamba, T.P. Burgin, G.M. Whitesides, D.L. Allara, A.N. Parikh, and S.V. Atre, J. Am. Chem. Soc. **117**, 9529 (1995); C.M. Fischer, M. Burghard, S. Roth, and K. v. Klitzing, Appl. Phys. Lett. **66**, 3331 (1995); E. Delamarche, B. Michel, H.A. Biebuyck, and C. Gerber, Adv. Mater. **8**, 718 (1996); L.A. Bumm, J.J. Arnold, M.T. Cygan, T.D. Dunbar, T.P. Burgin, L. Jones II, D.L. Allara, J.M. Tour, and P.S. Weiss, Science **271**, 1705 (1996); R.P. Andres, T. Bein, M. Dorogi, S. Feng, J.I. Henderson, C.P. Kubiak, W. Mahoney, R.G. Osifchin, and R. Reifenberger, *ibid.* **272**, 1323 (1996); M.A. Reed, C. Zhou, C.J. Muller, T.P. Burgin, and J.M. Tour, *ibid.* **278**, 252 (1997); S. Datta, W. Tian, S. Hong, R. Reifenberger, J.I. Henderson, and C.P. Kubiak, Phys. Rev. Lett. **79**, 2530 (1997); C. Zhou, M.R. Deshpande, M.A. Read, L. Jones II, and J.M. Tour, Appl. Phys. Lett. **71**, 611 (1997); S.J. Tans, M.H. Devoret, H. Doi, A. Thess, R.E. Smalley, L.J. Geerligs, and C. Dekker, Nature (London) **386**, 474 (1997); C. Joachim and J.K. Gimzewski, Chem. Phys. Lett. **265**, 353 (1997); C. Kergueris, J.-P. Bourgoin, S. Palacin, D. Esteve, C. Urbina, M. Magoga, and C. Joachim, Phys. Rev. B **59**, 12 505 (1999); Z. Yao, H.W.C. Postma, L. Balents, and C. Dekker, Nature (London) **402**, 273 (1999).

[2] V. Mujica, M. Kemp, and M. A. Ratner, J. Chem. Phys. **101**, 6849 (1994); **101**, 6856 (1994).

[3] E.G. Petrov, I.S. Tolokh, A.A. Demidenko, and V.V. Gorbach, Chem. Phys. **193**, 237 (1995).

[4] M. Magoga and C. Joachim, Phys. Rev. B **57**, 1820 (1998).

[5] A. Onipko, Yu. Klymenko, L. Malysheva, and S. Stafström, Solid State Commun. **108**, 555 (1998).

[6] A. Onipko, Phys. Rev. B **59**, 9995 (1999).

[7] M.P. Samanta, W. Tian, S. Datta, J.I. Henderson, and C.P. Kubiak, Phys. Rev. B **53**, R7626 (1996).

[8] M. Magoga and C. Joachim, Phys. Rev. B **56**, 4722 (1997).

[9] W. Tian, S. Datta, S. Hong, R. Reifenberger, J.I. Henderson, and C.P. Kubiak, J. Chem. Phys. **109**, 2874 (1998).

[10] H. Mehrez, S. Ciraci, A. Buldum, and I.P. Batra, Phys. Rev. B **55**, R1981 (1997).

[11] N.D. Lang and Ph. Avouris, Phys. Rev. Lett. **81**, 3515 (1998).

[12] A. Nakamura, M. Brandbyge, L.B. Hansen, and K.W. Jakobsen, Phys. Rev. Lett. **82**, 1538 (1999).

[13] R. Landauer, IBM J. Res. Dev. **1**, 323 (1957); Philos. Mag. **21**, 683 (1970).

[14] M. Büttiker, Y. Imry, R. Landauer, and S. Pinhas, Phys. Rev. B **31**, 6207 (1985).

[15] A.D. Stone and A. Szafer, IBM J. Res. Dev. **32**, 384 (1988).

[16] C. Caroli, R. Combescot, P. Nozieres, and D. Saint-James, J. Phys. C **4**, 916 (1971).

[17] S. Datta, *Electronic Transport in Mesoscopic Systems* (Cambridge University Press, Cambridge, England, 1995).

[18] M. Lannoo and P. Friedel, *Atomic and Electronic Structure of Surfaces* (Springer-Verlag, Berlin, 1991).

[19] M.-C. Desjonquéres and D. Spanjaard, *Concepts in Surface Physics* (Springer-Verlag, Berlin, 1993).

[20] D.M. Newns, Phys. Rev. **178**, 1123 (1969).

[21] A.I. Onipko, K.-F. Berggren, Yu.O. Klymenko, L.I. Malysheva, J.J.W.M. Rosink, L.J. Geerligs, E. van der Drift, and S. Radelaar, Phys. Rev. B **61**, 11 118 (2000).

[22] J. Bardeen, Phys. Rev. Lett. **6**, 57 (1961).

[23] H. Sellers, A. Ulman, Y. Shnidman, and J.E. Eilers, J. Am. Chem. Soc. **115**, 9389 (1993).

[24] A. Onipko, Yu. Klymenko, and L. Malysheva, Mater. Sci. Eng., C **8-9**, 281 (1999).

[25] J. Tersoff and D.R. Hamman, Phys. Rev. B **31**, 805 (1985).

[26] A.L. Vázquez de Parga, O.S. Hernan, R. Miranda, A. Levy Yeyati, N. Mingo, A. Martín-Rodero, and F. Flores, Phys. Rev. Lett. **80**, 357 (1998).

[27] N.D. Lang, Phys. Rev. B **34**, R5947 (1986).

[28] D.A. Papaconstantopoulos, *Handbook of the Band Structure of Elemental Solids* (Plenum, New York, 1986).

[29] L.I. Malysheva and A.I. Onipko, J. Phys.: Condens. Matter **7**, 3597 (1995).

[30] A. Levy Yeyati, A. Martín-Rodero, and F. Flores, Phys. Rev. B **56**, 10 369 (1997).

[31] Y. Xue, S. Datta, S. Hong, R. Reifenberger, J.I. Henderson, and C.P. Kubiak, Phys. Rev. B **59**, R7852 (1999).

[32] J.J.W.M. Rosink, M.A. Blauw, L.J. Geerligs, E. van der Drift, B.A.C. Rousseeuw, S. Radelaar, W.G. Sloof, and E.J.M. Fakkeldij, Langmuir **16**, 16 (2000).

[33] J.J.W.M. Rosink, M.A. Blauw, L.J. Geerligs, E. van der Drift, B.A.C. Rousseeuw, and S. Radelaar, Mater. Sci. Eng., C **8-9**, 267 (1999).

[34] Å. Johansson and S. Stafström, Chem. Phys. Lett. **322**, 301 (2000).

[35] A. Onipko, Chem. Phys. Lett. **292**, 267 (1998).

[36] A. Onipko and Yu. Klymenko, J. Phys. Chem. A **102**, 4246 (1998).

[37] B.A. Lippmann, Phys. Rev. Lett. **15**, 1 (1965); **16**, 135 (1966).

[38] R.L. Kronig, J. Opt. Soc. Am. Rev. Sci. Instrum. **12**, 547 (1926).

[39] H.A. Kramers, Atti. Congr. Intern. Fisici Como **2**, 545 (1927).

[40] D.N. Zuberev, *Neravnovesnaya Statisticheskaya Termodinamika* (Moskva, Nauka, 1971).

[41] J.H. Davies *The Physics of Low-Dimensional Semiconductors. An Introduction* (Cambridge University Press, Cambridge, England, 1998).

[42] J. Cerdá, M.A. Van Hove, P. Sautet, and M. Salmeron, Phys. Rev. B **56**, 15 885 (1997).